Supplementary Information for

Ab initio modeling of oxygen vacancies and protonic defects in $La_{1-x}Sr_xFeO_{3-\delta}$ perovskite solid solutions

D. Gryaznov*[a], R. Merkle[b], E. A. Kotomin[a,b], J. Maier[b]
[a]Institute for Solid State Physics, University of Latvia, Riga, Latvia
[b]Max Planck Institute for Solid State Research, Stuttgart, Germany

(1) Mulliken charges and magnetic moments

Table S1: Mulliken charges, magnetic moments and Fe-O distances (averaged over the FeO_6 octahedron)

L4S4F8O24: each O has two Sr and two La neighbors in its first coordination shell

atom	average Fe-O / Å	magn. mom. / μ_B	Charge / *e*	formal ox. state			
9 (Fe)	1.991	4.22	2.236	3+			
10 (Fe)	1.991	4.22	2.236	3+			
11 (Fe)	1.997	4.276	2.243	3+			
12 (Fe)	1.997	4.276	2.243	3+			
13 (Fe)	1.947	3.831	2.232	4+			
14 (Fe)	1.947	3.831	2.232	4+			
15 (Fe)	1.948	3.803	2.218	4+			
16 (Fe)	1.948	3.803	2.218	4+			
atom	charge / *e*	atom	charge / *e*	atom	charge / *e*	atom	charge / *e*
1 (Sr)	1.917	17 (O)	-1.462	25 (O)	-1.586	33 (O)	-1.487
2 (Sr)	1.917	18 (O)	-1.462	26 (O)	-1.586	34 (O)	-1.487
3 (Sr)	1.919	19 (O)	-1.473	27 (O)	-1.551	35 (O)	-1.589
4 (Sr)	1.919	20 (O)	-1.473	28 (O)	-1.551	36 (O)	-1.589
5 (La)	2.658	21 (O)	-1.458	29 (O)	-1.488	37 (O)	-1.557
6 (La)	2.651	22 (O)	-1.458	30 (O)	-1.488	38 (O)	-1.557
7 (La)	2.651	23 (O)	-1.466	31 (O)	-1.574	39 (O)	-1.430
8 (La)	2.643	24 (O)	-1.466	32 (O)	-1.466	40 (O)	-1.430

L7S1F8O24: n_{Sr} is the number of Sr in the first coordination shell of the O

atom	average Fe-O / Å	magn. mom. / μ_B	charge / *e*	formal ox. state			
9 (Fe)	2.008	4.344	2.258	3+			
10 (Fe)	1.959	3.848	2.241	4+			
11 (Fe)	2.010	4.345	2.260	3+			
12 (Fe)	2.007	4.348	2.259	3+			
13 (Fe)	2.008	4.348	2.260	3+			
14 (Fe)	2.008	4.299	2.252	3+			
15 (Fe)	2.009	4.287	2.250	3+			
16 (Fe)	2.008	4.347	2.259	3+			
atom	charge / *e*	atom, n_{Sr}	charge / *e*	atom, n_{Sr}	charge / *e*	atom, n_{Sr}	charge / *e*
1 (La)	2.650	17 (O) 0 Sr	-1.635	25 (O) 1 Sr	-1.628	33 (O) 2 Sr	-1.620
2 (La)	2.644	18 (O) 0 Sr	-1.508	26 (O) 0 Sr	-1.598	34 (O) 2 Sr	-1.484
3 (La)	2.643	19 (O) 0 Sr	-1.612	27 (O) 0 Sr	-1.614	35 (O) 0 Sr	-1.632
4 (La)	2.544	20 (O) 1 Sr	-1.634	28 (O) 0 Sr	-1.632	36 (O) 0 Sr	-1.634
5 (La)	2.544	21 (O) 1 Sr	-1.634	29 (O) 0 Sr	-1.621	37 (O) 0 Sr	-1.624
6 (La)	2.651	22 (O) 1 Sr	-1.514	30 (O) 0 Sr	-1.478	38 (O) 0 Sr	-1.593
7 (Sr)	1.916	23 (O) 1 Sr	-1.611	31 (O) 0 Sr	-1.636	39 (O) 0 Sr	-1.631
8 (La)	2.646	24 (O) 1 Sr	-1.634	32 (O) 2 Sr	-1.636	40 (O) 0 Sr	-1.631

L4S4F8O23:

atom	average Fe-O / Å	magn. mom. / μ_B	charge / *e*	formal ox. state			
9 (Fe)	2.010	4.246	2.204	3+			
10 (Fe)	1.957	3.800	2.228	4+			
11 (Fe)	1.951	3.838	2.235	4+			
12 (Fe)	2.021	4.345	2.257	3+			
13 (Fe)	2.018	4.295	2.248	3+			
14 (Fe)	1.997	4.236	2.237	3+			
15 (Fe)	2.005	4.289	2.245	3+			
16 (Fe)	1.989	4.239	2.203	3+			
atom	charge / *e*	atom	charge / *e*	atom	charge / *e*	atom	charge / *e*
1 (Sr)	1.915	17 (V)	0.237	25 (O)	-1.583	33 (O)	-1.607
2 (Sr)	1.918	18 (O)	-1.612	26 (O)	-1.477	34 (O)	-1.483
3 (Sr)	1.913	19 (O)	-1.571	27 (O)	-1.466	35 (O)	-1.490
4 (Sr)	1.914	20 (O)	-1.642	28 (O)	-1.616	36 (O)	-1.615
5 (La)	2.625	21 (O)	-1.595	29 (O)	-1.577	37 (O)	-1.602
6 (La)	2.628	22 (O)	-1.492	30 (O)	-1.568	38 (O)	-1.492
7 (La)	2.656	23 (O)	-1.468	31 (O)	-1.574	39 (O)	-1.503
8 (La)	2.648	24 (O)	-1.591	32 (O)	-1.584	40 (O)	-1.626

L4S4F8O24H: H is attached to O29

atom	average Fe-O / Å	magn. mom. / μ_B	charge / *e*	formal ox. state			
9 (Fe)	Fe-O 1.982	4.269	2.228	3+			
	Fe-OH 2.172						
10 (Fe)	2.016	4.290	2.244	3+			
11 (Fe)	1.995	4.248	2.239	3+			
12 (Fe)	1.996	4.236	2.239	3+			
13 (Fe)	Fe-O 1.988	4.320	2.237	3+			
	Fe-OH 2.194						
14 (Fe)	1.952	3.779	2.227	4+			
15 (Fe)	1.951	3.815	2.231	4+			
16 (Fe)	1.955	3.842	2.236	4+			
atom	charge / *e*	atom	charge / *e*	atom	charge / *e*	atom	charge / *e*
1 (Sr)	1.912	17 (O)	-1.581	25 (O)	-1.483	33 (O)	-1.568
2 (Sr)	1.919	18 (O)	-1.574	26 (O)	-1.605	34 (O)	-1.456
3 (Sr)	1.918	19 (O)	-1.587	27 (O)	-1.500	35 (O)	-1.462
4 (Sr)	1.918	20 (O)	-1.576	28 (O)	-1.487	36 (O)	-1.479
5 (La)	2.651	21 (O)	-1.474	29 (O)	-1.194	37 (O)	-1.590
6 (La)	2.632	22 (O)	-1.577	30 (O)	-1.609	38 (O)	-1.473
7 (La)	2.643	23 (O)	-1.485	31 (O)	-1.576	39 (O)	-1.472
8 (La)	2.652	24 (O)	-1.465	32 (O)	-1.577	40 (O)	-1.481
						41 (H)	0.204

(2) Partial density of states (DOS) for Fe, O and H states calculated with the PBE0 hybrid functional. We follow the same approach as suggested in ref. 1 and align the low lying O 2s states to the same energy in all calculated DOS.

a)

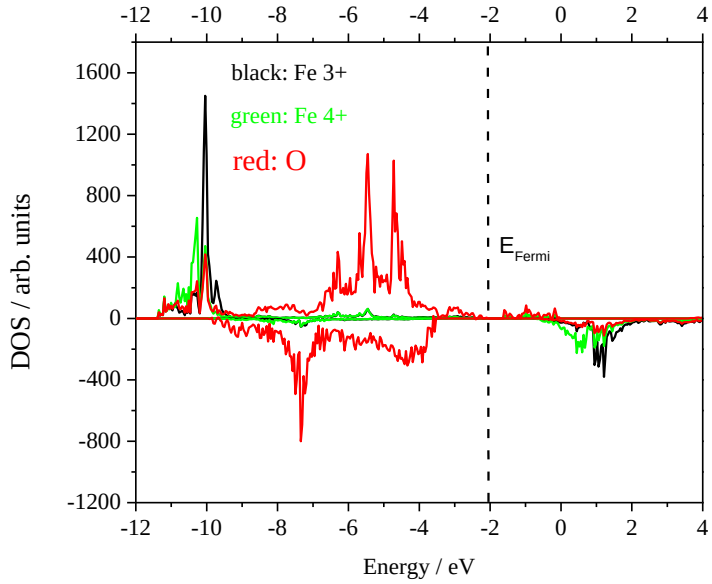

b)

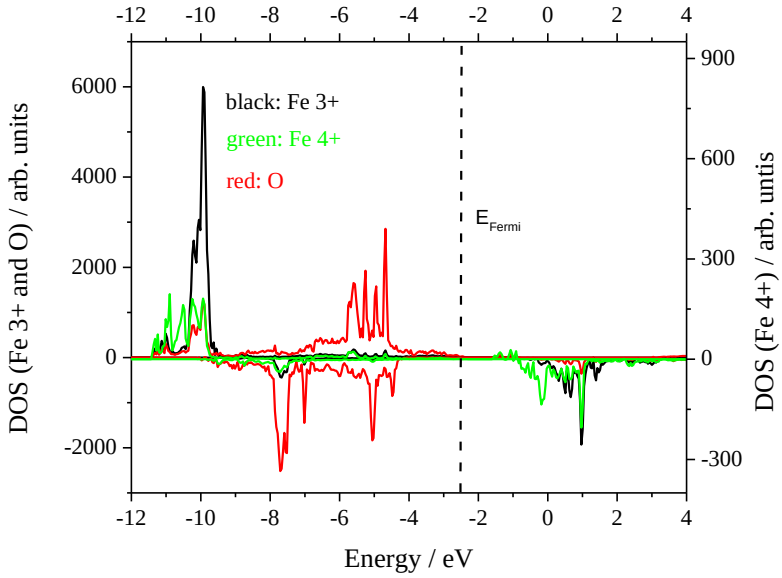

c)

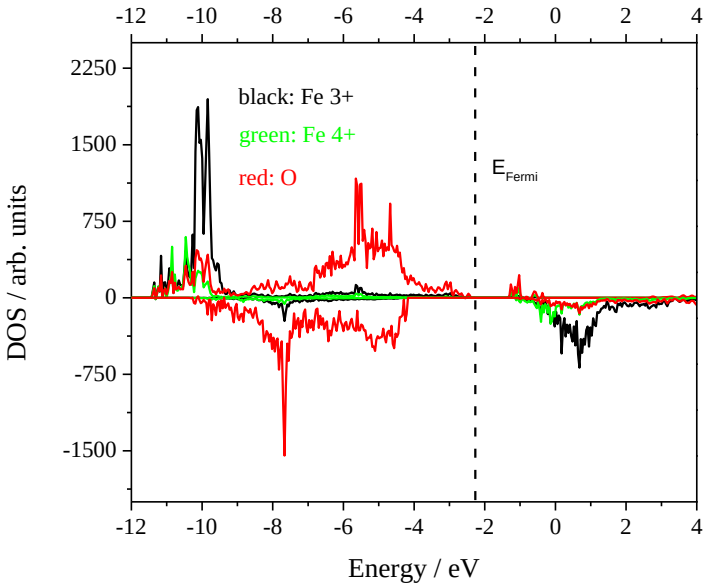
black: Fe 3+
green: Fe 4+
red: O
E_Fermi
DOS / arb. units
Energy / eV

d)

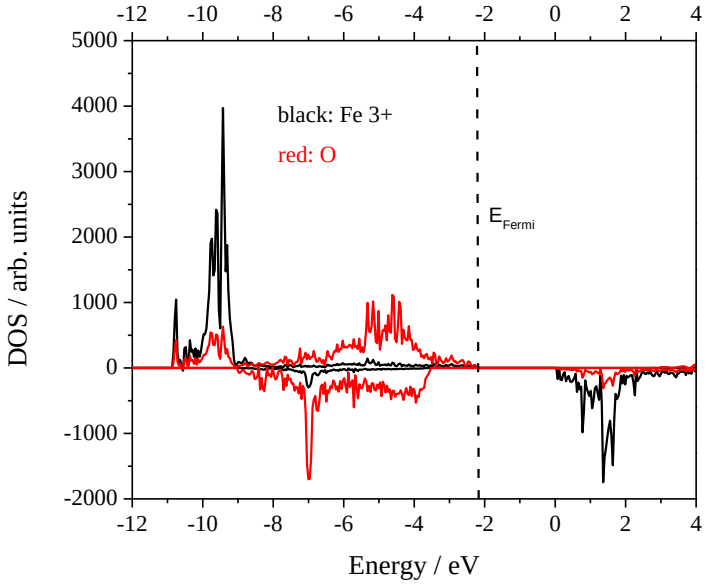
black: Fe 3+
red: O
E_Fermi
DOS / arb. units
Energy / eV

e)

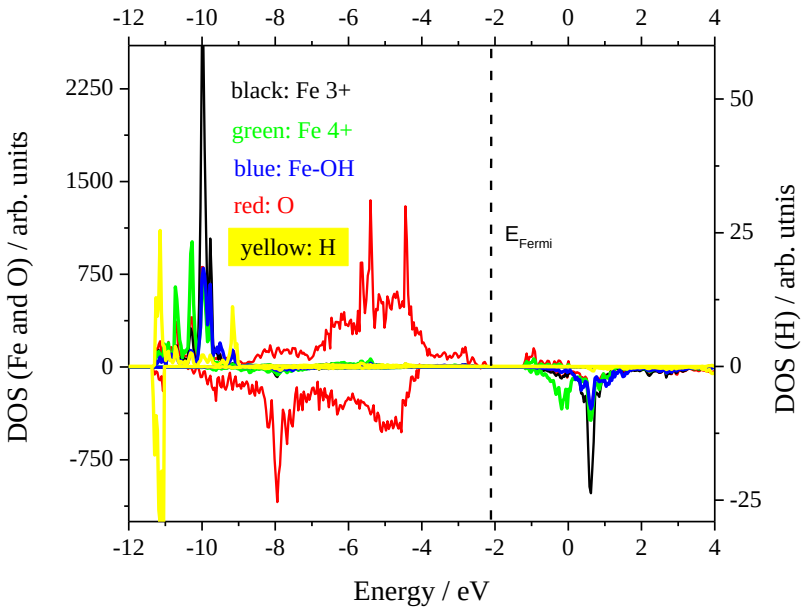

Figure S1: The partial DOS for L4S4F8O24 (a), L7S1F8O24 (b), L4S4F8O23 (c), L4S4F8O22 (d), L4S4F8O24H (e). The DOS for spin down electrons is represented by negative values. Dashed lines indicate the relevant Fermi energies. The energy scale is adjusted by aligning the O2s electrons (not shown) of all systems to the same value. The energy value difference between two grid points is 0.04 eV. Notice different scaling for Fe^{4+} in L7S1F8O24 and H in L4S4F8O24H due to their small number in supercells.

Comparing (a), (c) and (d) which represent an increasing oxygen deficiency in $La_{0.5}Sr_{0.5}FeO_{3-\delta}$, one can recognize that the "center of gravity" of the DOS of Fe and O gradually moves to higher energies, corresponding to a lower average Fe oxidation state.

(3) Comparison of formation energies from different *ab initio* methods

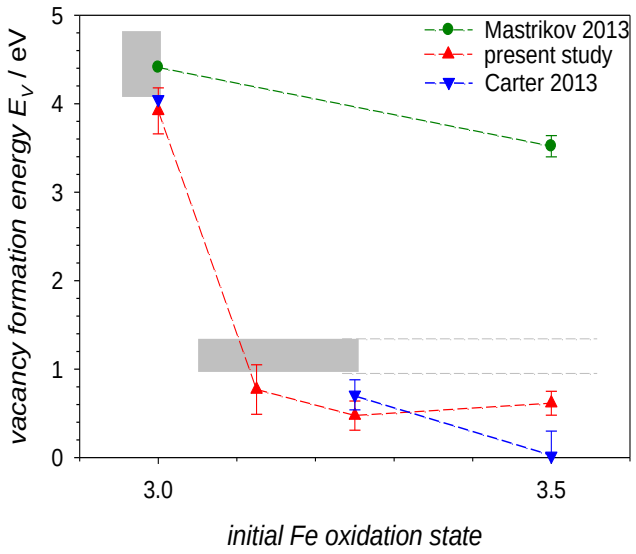

Figure S2: Oxygen vacancy formation energies in $La_{1-x}Sr_xFeO_{3-\delta}$ ($0 \leq x \leq 0.5$) as function of initial Fe oxidation state. The gray boxes indicate the experimental values of vacancy formation energy for Fe oxidation state between 2+ and 3+ and the much lower value between Fe^{3+} and Fe^{4+}, taken from ref. 2. green circles: $LaFeO_{3-\delta}$ and $La_{0.5}Sr_{0.5}FeO_{3-\delta}$ from ref. 3 calculated with GGA, pseudocubic 40-atom supercell (the "error bar" gives the energy rage resulting from different local atomic configurations around the vacancy). Blue triangles: $La_{1-x}Sr_xFeO_{3-\delta}$ (x = 0, 0.25, 0.5) from ref. 4 calculated with GGA+U functional (pseudocubic 40-atom supercell, U = 4.3 eV). red triangles: present this study with hybrid PBE0 functional (rhombohedral 40-atom supercell). As one can see, only the latter reproduces the experimental trend of the vacancy formation energy vs Fe oxidation state due to a proper treatment of the electron correlation effects. Note also that this energy is very sensitive to the proper treatment of the symmetry of perfect and defective supercells involved in its calculations. The symmetry aspects explain the very small formation energies for $La_{0.5}Sr_{0.5}FeO_{3-\delta}$ as discussed in refs. 4-5 whereas the present study demonstrates the role of distortion effects.

References

1 E. A. Kotomin, Yu. A. Mastrikov, M. M. Kuklja, R. Merkle, A. Roytburd, J. Maier, Solid State Ionics 2011, **188**, 1-5

2 J. Mizusaki, M. Yoshihiro, S. Yamauchi, K. Fueki, J. Sol. State Chem. 1987, 67, 1-8

3 Y. A. Mastrikov, R. Merkle, E. A. Kotomin, M. M. Kuklja, J. Maier, *Phys. Chem. Chem. Phys.* 2013, **15**, 911-918

4 A. B. Ritzmann, A. Muñoz-García, M. Pavone, J. A. Keith, E. A. Carter, *Chem. Mater.* 2013, **25**, 3011-3019

5 D. Gryaznov, S. Baumann, E . A. Kotomin, R. Merkle, *J. Phys. Chem.* C 2014, **118**, 29542-29553